SEASONAL DRIVERS OF AMPLITUDE PATTERNS IN A POPULATION OF RED-BACKED VOLES (CLETHRIONOMYS RUTILUS)

By

Sarah Swanson, B.A.

A Thesis Submitted in Partial Fulfillment of the Requirements

for the degree of

Master of Science

In

Wildlife Biology and Conservation

University of Alaska Fairbanks

August 2023

APPROVED

Knut Kielland, Committee Chair
Shawn Crimmins, Committee Member
Diane Wagner, Committee Member
Melanie Flamme, Committee Member
Todd Brinkman, Program Chair
Wildlife Biology & Conservation
Karsten Hueffer, Dean
College of Natural Science and Mathematics
Richard Collins, Director
Graduate School

Abstract

Northern red-backed voles (*Clethrionomys rutilus*) are an important species in the Interior Alaska boreal forest ecosystem, both as important herbivores and as a key food source for many mammalian and avian predators. However, they exhibit dramatic inter- and intra-annual population fluctuations, for which causes are not entirely known. Winter mortality is often very high and altered weather conditions due to climate change, such as rain on snow or delayed snowfall in autumn, may increase stress during an already difficult season. These considerations prompted this investigation into overwinter survival of northern red-backed voles in Denali National Park and Preserve, with the goal of examining a time series of population densities and assessing how weather variables influenced patterns of mortality. Using a 30-year record of mark-recapture data, I applied spatially-explicit methods to calculate density estimates for autumn and early summer trapping sessions. I also assessed cyclic behavior and used post-hoc linear modeling to examine patterns in amplitude and period of population fluctuations. I found that this microtine population appears to be cycling on a 2-4 year period, with some differentiation among sampling sites. Models of autumn amplitudes suggested a linkage between white spruce (*Picea glauca*) seed mast, either an important source of food during winter seasons, or as a coincidental product of the underlying multi-annual environmental triggers that promote high seed fall. I also found a negative effect of combined late snowfall and cold temperatures, a scenario that may become more prominent under future climate changes. Lastly, my models of early summer density showed an apparent negative density dependence, in which high population densities in autumn were followed by low densities the following spring. Continued monitoring of voles, alongside more thorough assessments of snow conditions, habitat, diet, and predator status would assist further attempts to cast light upon the complex population dynamics of this species and their many predators.

Keywords: *Myodes rutilus*, *Clethrionomys rutilus*, Alaska, boreal forest, Denali National Park and Preserve, density dependence, cyclicity, northern red-backed vole, spruce mast

Table of Contents

Page

List of Figures Page

List of Tables Page

List of Appendices Page

Acknowledgements

First, I would like to thank my advisor and committee members for their guidance throughout the past years. I would also like to thank Josh Schmidt, Derek Arnold, David Swanson, and Greg Breed for their assistance with statistical analysis, Dominique Fautuex and Matthew Cameron for contributing code, and Christa Mulder and Shelli Swanson for their helpful critiques of the manuscript. I was extremely fortunate to have wonderful friends within and outside my graduate student cohort, and am forever grateful for their collaboration and support. In addition to serving as a committee member, Melanie Flamme has served as the primary investigator for the small mammal project on which this thesis is based since 2005, and is an integral part of this research. Funding for this project was provided by the U.S. National Park Service, both from Denali National Park and Preserve and the Central Alaska Inventory and Monitoring Network, in addition to generous support from the Ted McHenry Biology Field Research Fund. Lastly, I would like to express my gratitude to the many technicians, volunteers, and employees who persevered through rain and shine to collect this data; without you, none of this would be possible.

1. Introduction

Small mammals serve as both a vital, resident prey base and prominent herbivores in the boreal ecosystem, and thus have a substantial impact on trophic dynamics year-round (Hanski et al. 2001, Gilg et al. 2003, 2009, Ims and Fuglei 2005). However, voles can be a wildly fluctuating food source, with populations varying dramatically both between and within years (Boonstra and Krebs 2012, Cornulier et al. 2013, Mihok et al. 2019, Fauteux et al. 2021). These population fluctuations directly affect a variety of avian and mammalian predators, so understanding these trends is of utmost importance for understanding food webs in boreal regions (Ims and Fuglei 2005).

Factors influencing population levels of small rodents include a suite of physical and biological factors, the relative importance of which have been a topic of debate for decades. In some geographic areas voles and lemmings exhibit cyclic populations that peak every 3-5 years (Krebs and Myers 1974, Stenseth 1999, Fauteux et al. 2015), while in other populations those patterns are muted (Boonstra and Krebs 2012) or disappearing as a possible result of climate change (Ims et al. 2008, Cornulier et al. 2013, but see Korpela et al. 2013). Drivers of these cyclic fluctuations are not well understood, but the most common explanations are predation (Hanski et al. 2001, Klemola et al. 2002, Korpimäki et al. 2002) or maternal effects (Boonstra et al. 1998a, Ginzburg and Krebs 2015). The latter can take the form of altered growth rate (animals born in high years grow more quickly than those born in a decline) or reproductive capacity, indicated by prolonged stress responses affecting body mass and reproductive hormone response (Boonstra et al. 1998b, Sundell et al. 2019). Amplitudes of these cycles (or abundances for non-cyclic populations) appear to be influenced by numerous factors, including food availability (Elias et al. 2006, Krebs et al. 2010, Johnsen et al. 2017, Schmidt et al. 2017), predator interactions (Ginzburg and Krebs 2015), and climate (Korslund and Steen 2006, Gilg et al. 2009, Bilodeau et al. 2013, Domine et al. 2018). Climate change is occurring at a rapid rate in North American boreal forest regions (Overland et al. 2019), and the effects on small-mammal cyclic dynamics have remained mostly unstudied. Thus, understanding the direct and indirect effects of climate change on small mammals in interior Alaska is critical.

Prominent signs of climate change in interior Alaska are altered winter conditions, including higher temperatures, shorter snow season, and variable snow fall (Littell et al. 2018, Overland et al. 2019, Lader et al. 2020). Changing winter conditions are known to disrupt multiple trophic levels within high-latitude ecosystems (Terraube et al. 2015, Penczykowski et al. 2017) and may be particularly significant for small mammals. Overwinter survival is a limiting factor for red-backed vole populations, for which a decrease of 50% or more during the colder months is not uncommon (Boonstra and Krebs 2012). Snow conditions directly affect survival by influencing capacity to escape predators (Lindström and Hörnfeldt 1994), find food (Korslund and Steen 2006, Gilg et al. 2009), and avoid thermal stress, especially hypothermia (Bilodeau et al. 2013). To fulfill these needs, snow must be sufficiently deep to provide insulation (Duchesne et al. 2011), of low density near the ground to ensure mobility and food accessibility, and long-lasting enough to offer the previous benefits for the duration of winter (Bilodeau et al. 2013).

Other snow-related obstacles to vole survival are rain-on-snow events, which are predicted to become more frequent in Alaska under climate change scenarios (Rennert et al. 2009). Such events may limit vole mobility and food accessibility by fragmenting the subnivean space, increasing snow density, and coating food sources in ice (Ims and Fuglei 2005, Bilodeau et al. 2013, Soininen et al. 2015, Berteaux et al. 2017). This could also increase vole metabolic demands by reducing the insulative value of the snowpack and possibly even their own fur if unable to stay dry (Berteaux et al. 2017). A more thorough analysis of winter conditions and their ramifications for voles would aid in predicting how their populations may respond to more varied winter weather. However, assessing the impacts of such conditions on small mammal population dynamics is challenging due to the data needs and complexities associated with understanding the drivers of cyclical populations.

To address this issue, I analyzed 30 years of northern red-backed vole population data in Denali National Park and Preserve. Previous worked suggested that voles in this area retained cyclical dynamics as recently as 2014 (Schmidt et al. 2017). However, recent population crashes suggest that the cyclical dynamics of voles in this region may be disrupted by weather and winter conditions. I examined ways in which abundances of northern red-backed voles are coupled to

weather and temperature regimes. I hypothesized that parameters such as low summer primary productivity, warm weather events during the winter, limited snow fall, and shorter snow season could negatively impact vole populations by reducing abundance. Lastly, I used an abbreviated dataset in which density estimates for both autumn and the following early summer could be calculated to explore climate factors affecting winter population dynamics, from which I predicted that late snowfall and ice layers in the snowpack would be followed by low spring vole population densities.

2. Methods

2.1 Study Site

This study was conducted in the Rock Creek drainage of Alaska's Denali National Park and Preserve, at approximately 62.730, -149.985 and elevation 735 m. The site was established as a Long Term Ecological Monitoring (LTEM) location by the National Park Service (NPS), University of Alaska Fairbanks, and United States Geological Survey (USGS) in 1992 (Oakley and Boudreau 2000, Rexstad et al. 2005). Since 2005, the project has been managed by the Central Alaska Inventory and Monitoring Network (Maccluskie and Oakley 2003). My field site has a continental climate characterized by short, warm summers and long, cold winters (Figure 1).

Typically, only five months (May – September) have average monthly temperatures above 0 °C. July, the warmest month, has an average monthly temperature of 13 °C; whereas January is the coldest month, at -16 °C (Sousanes and Hill 2018). The Alaska Range, which lies mostly south of the Rock Creek site, acts as a barrier to warm, moist air flowing northward from the Gulf of Alaska and causes relatively low annual precipitation, averaging approximately 380 mm per year. Low snow depths (mean snowfall of 1.95 m per winter, but mean snow depth of 0.3 m due to sublimation and thaw), coupled with an annual average temperature of -2.3 °C, causes the area to have permafrost (Sousanes and Hill 2015).

Small-mammal sampling has been carried out at four 100-by-100 m plots in the Rock Creek drainage, two in a riparian area and two on an adjacent ridge in forest (Figure 2). To describe habitat, I used data from three vegetation monitoring plots set within each small mammal trapping grid (see Roland et al. 2004 for data collection process). The forested grids were located in an area of sparse white spruce (*Picea glauca*, 5.6 m^2/ha live basal area) and occasional black spruce (*P. mariana*, 0.05 m^2/ha). Trees were underlain with mosses (mean cover 69%), Bigelow's sedge (*Carex bigelowii*, 17%), blueberries (*Vaccinium uliginosum* 11%), shrub birch (*Betula nana*, 10%), low-bush cranberries (*V. vitus-idea*, 10%), Labrador tea (*Rhododendron groenlandicum*, 10%) and other small shrubs (Figure 3, A and B, Table 1). The south-west corner of Forest 1 (F1) contains a drainage path characterized by uneven ground and dense willows, while Forest 2 (F2) is largely consistent (Figure 2).

Despite having nearly similar cover, trees are larger and denser on the riparian plots (white spruce, 13m^2/ha) and black spruce are absent. Riparian plots contain a higher species richness of graminoids (six spp., three on forest plots) and forbs (nine spp., one on forest plot) (Figure 3, C and D). Riparian 1 (R1) contains a thick stand of alder covering the western-most fifth of the plot and similarly dense willows covering the eastern-most fifth. Approximately half of Riparian 2 (R2) overlaps a meadow that is often covered by overflow (aufeis in the winter and early spring (Figure 3, D).

2.2 Field Methods

Small-mammal populations are monitored annually by NPS as part of a long-term monitoring program, established in 1992. Plots monitored have varied over the years (Table 2). I used data beginning in autumn of 1993 to allow for a pilot session in 1992 during which trap checks were conducted less frequently. To assess the effects of overwinter survival, I used data from paired trapping sessions that occurred in the autumn and early summer of the following year. Autumn trapping took place during the second week of August for all years (1993-2022), when voles had not yet begun to experience winter mortality and were at their peak population for the year. Early summer trapping was conducted during the second or third week of June in

1994-2003 and 2020-2022. This schedule was chosen to limit overnight mortality due to cold temperatures and avoid late snowfall.

During trapping sessions, each of the four plots contained 100 Sherman live-traps arranged in a 10-by-10 grid, spaced approximately 10 m apart. Traps were protected by plastic covers to keep animals dry in the rain and shaded from sun. They were baited with sunflower seeds and stocked with two cotton nestlets, which animals could shred and use to make nests for warmth. Traps were checked three times a day (06:00, 13:00, 20:00) for four consecutive days. Each animal was scanned upon capture by a Passive Integrative Transponder (PIT) tag reader to establish capture status, marked or unmarked. Each unmarked animal had a 9-12mm PIT tag injected into their subcutaneous fat, establishing their individual identities used in the mark-recapture techniques. Trapping and handling was conducted according to the guidelines of the American Society of Mammalogy, and procedures were approved by the NPS institutional animal care and use committee (IACUC, protocol identifier AK_DENA_Swanson_Vole.Shrew_2020.A1). Further plot set up and detailed trapping procedures can be found in the NPS Small Mammal Monitoring Protocol for Central Alaska Network and associated SOPs (Flamme et al. 2018).

2.3 Covariates

2.3.1 Density Dependent Terms

My first category of covariates was chosen to represent potential cyclic or density-dependent patterns. Given past research (Schmidt et al. 2017) and results from my own autocorrelation assessments (see below), I included sine and cosine waves with various period length to provide a generalized cycle, combined to account for variation in cycle. in addition to lagged density estimations from past years. To adjust for missing data points caused by a flooding creek blocking access to forest plots (2019), this covariate was populated using a linear model quantifying the relationship between densities on forest plots and riparian plots in other high years (2002, 2005, 2008, 2009, 2011, 2014, 2017, 2021, and 2022). R2 showed the best correlation with forest plots, and was thus used to estimate the lag year covariate. To account for

the somewhat extreme variation in density estimates, I also used a binary version of lagged density that categorized the previous year as high or low, with a density of 10 voles/ha chosen as the threshold between categories based on preliminary plotting.

2.3.2 Climate

I obtained weather data from a station near NPS Headquarters, located approximately 1.6 km from my study area. To assess application of this data source to my specific study sites, I examined preliminary results from an ongoing study of variability in snow depth within the lower Rock Creek watershed (S. Stehn, personal communication, Jan 2023). For that study, three snow plots were located near the small mammal trapping grids and monitored for four winter seasons (2019-2023). Each snow plot consisted of a 20 x 20 m grid of ~50 snow depth measurements. In general, I determined that measurements taken from the weather station were sufficiently representative to be used for my analysis, particularly considering the need for a consistent source of weather data across my thirty-year time span. However, I would like to acknowledge the following differences: Across years, snow depths at R2 were comparable to the weather station until early spring, when melt occurred faster in the southern aspect, open meadow area than the flat, shaded weather station. Depths recorded at the snow plot near R1 were generally up to 10 cm higher than those from the weather station until February, after which they were consistent with weather station data. The snow site near F1 showed that forest plots generally had more snow than the weather station, ranging between 10-20 cm higher during the first half of the winter to only 0-10cm higher after February (S. Stehn, personal communication, Jan 2023). Despite these differences, I concluded that a majority of the year-to-year variation and magnitude in snow depth was captured by the long-term monitoring site.

All snow-related variables were measured daily during the snow year, defined as the period between the last day in a calendar year with snow depth = 0cm (snow-on date) and first day of the following spring when snow depth = 0cm (snow-off date). I selected variables for analysis based on the potential for thermal stress (due to late or little snowpack), limited mobility (due to snow compaction or ice layers resulting from temperatures above freezing), and food availability for voles (Table 3). I used melt and rain days as proxies for icing and compaction in

the snowpack, while autumn harshness reflected the amount of thermal stress that voles could be exposed to before sufficient snow insulation was established. Using data from the weather station, I created several precipitation variables and calculated growing degree days (GDD) to represent growing conditions present during the main reproductive season. The combination of GDD, cumulative summer precipitation, and mean snow depth has been shown explain most of the variation in average annual maximum Normalized Difference Vegetation Index (NDVI), a common proxy for primary productivity, across the same time period (Schmidt et al. 2017). Rather than using a five-year moving average, I chose to use a three-year moving average to better align with the short generation times in vole populations while also accommodating the initiation period for white spruce mast (Roland et al. 2014). For variables representing the growing season leading up to a trapping session, a cut-off of August 1st was used to restrict weather events to only those that would have affected animals prior to monitoring.

2.3.3 Spruce Seeds

I also included white spruce seed fall as a covariate, based on other species of vole and mice appearing to use spruce seeds as food sources (Elias et al. 2006, Falls et al. 2007). Seeds are collected at 3 plots near my sampling site, each of which contained 6 seed trays left out over winter (see Roland et al. 2014 for details on spruce seed collection). I took a mean of these measurements to calculate a covariate representing seeds present. Seeds attributed to a given year were those that fell the previous autumn and would be available as a food resource throughout the preceding winter.

2.4 Analytical Methods

2.4.1 Autumn Density

I conducted my analyses in two stages. First, I used a spatially-explicit capture recapture (SECR) approach to generate annual estimates of autumn densities for each plot. Then I conducted a post-hoc analysis using those density estimates as response variables in a linear modeling framework. I chose this two-stage approach because it allowed for an efficient model

selection process and has been used in previous research evaluating climatic effects on small mammal density (Fauteux et al. 2015, 2021, Bogdziewicz et al. 2016).

I chose spatially-explicit modeling over non-spatial methods to accommodate heterogeneity in capture probability and provide a more appropriate geographic boundary for the sampling area, which reduces density estimate bias (Efford and Fewster 2013). The observations, y_{ij}, for i = 1, 2, …, n captured individuals and j = 1, 2, …, J traps are a function of the number of sampling occasions, K, and encounter probability (p_{ij}) which can be expressed as (Royle et al. 2014):

$$y_{ij} \sim Binomial(K, p_{ij}) \qquad \text{Equation 1}$$

where p_{ij} can be written as:

$$p_{ij} = g_0 exp\left(-\frac{d^2}{2\sigma^2}\right) \qquad \text{Equation 2}$$

where detection probability (g_0) ≤ 1, d is the distance between the location of home range center and the location of trap and σ is a shape parameter representing the average home range size. I reduced truncation bias by constraining the potential area from which individuals might be exposed to traps (Efford 2020). To accomplish this, I set my buffer to 120m, which corresponds to the maximum calculated 4σ, following the recommendation of Efford (2020).

I modeled density in each plot separately due to the convergence issues associated with a single model fit to data from all 4 plots (results not shown). I fit six different models to capture histories from each plot, all of which included variation in density (D) by year. I included three options for g_0: a null model, a model that included variation by year, and a model that included a two-class mixture representing individual heterogeneity, essentially classifying an animal as either trap-happy or trap-shy. Lastly, I set σ to either be constant or to vary by year, representing a tendency for different home-range size given population levels. These models were then

compared using AICc values (Burnham and Anderson 2002). I fit all models using the SECR package (version 4.3.1) in program R, version 4.0.2 (Efford and Fewster 2013, Efford 2020).

Based on prior analysis, which showed a cyclic pattern with a period of roughly 3 years (Schmidt et al. 2017), I wanted to revisit the issue of cyclicity to accurately examine density dependent patterns. I plotted the annual estimates for each plot using the acf function (R statistical package), with any missing years of data excluded. I also fit a second-order log-linear model to assess direct and delayed density dependence and trends in cyclicity over time (Royama 1992, Bjornstad et al. 1995, Stenseth 1999, Ims et al. 2008, Fauteux et al. 2015). This model can be written as:

$$x_t = \beta_0 + (1 + \beta_1)x_{t-1} + \beta_2 x_{t-2} \qquad \text{Equation 3}$$

where, x_t represents log-transformed vole density at year t. β_0 is the intercept, and the first order term $(1+\beta_1)$ represents the coefficient for direct density dependence in year t-1, which could take the form of population self-regulation or a predator response. The second order term (β_2) represents the coefficient for delayed density dependence in year t-2, such as a less rapid predator response or increased pathogens in the population. The size of these coefficients indicates the influence of past years' densities on current year density. These terms for each plot were displayed on a phase plane diagram (Fauteux et al. 2015). This plot distinguishes between cyclic and non-cyclic populations, and further predicts period length for those that fall in the cyclic realm (see Royama 1992 for statictical explanation, Ims et al. 2008 for figure description).

For the second stage of the analysis, I used the density estimates from the SECR analysis for a series of post-hoc linear regressions using R statistical lme4 package (version 1.1-26) for mixed effect models. The general structure of these models was as follows:

$$D_{ts} \sim C_v \alpha + e_t \qquad \text{Equation 4}$$

in which density at year t and at plot s was modeled by a vector of covariates (C_v), their associated coefficients (α), and a random effect adjustment for year (e_t). To accommodate error

in SECR-produced density estimates, I constructed a bootstrapped dataset in which each year/plot included 1000 density estimates selected randomly from a distribution created using calculated means and standard errors. I truncated the distributions at 0 so that negative densities would not be included. These bootstrapped density values were then used as response variables for linear models, for which predictor variables included a variety of weather-related and density dependent factors (Table 3). All density estimates were log transformed for normality and all response variables were scaled using the scale() function to standardize the magnitude of effects and make comparisons of covariates more straightforward. For each of the 1000 iterations, the models in a given series were ranked based on AICc values to determine best fit (Burnham and Anderson 2002), creating a final summary table including average model rank, standard deviation of model rank, and average ΔAICc.

Given the variation in time between population peaks shown in the autocorrelation and phase plane plots, the second stage of the modeling process was comprised of two steps: modeling density dependence, and adding environmental effects. Modeling density dependence included sine and cosine terms with two or three-year periods, as well as a model with no density dependent effects. In preliminary trials, up to three years of lagged autumn density estimates were included to test the efficacy of using past data rather than a prescribed cycle length. However, this method required a shortened dataset to accommodate lag years and did not perform better than sine and cosine waves; thus only a single year lag term (AutumnEst, in Table 3) was used for the main analysis. To accommodate for this lagged density, the years represented in the linear models begin in 1994 rather than 1993 for F1 and R2, and in 1998 for R1 and F2. When previous years' densities were included as model covariates, estimates were taken from a bootstrapped distribution created through the same method described earlier for response densities, then log-transformed. A random effect representing unexplained variation between years was also added. The second step of model selection included the iterative addition of the sixteen environmental variables. This included the group of three variables which had been previously used to account for accumulated changes in NDVI, which serves as a proxy for primary productivity (See Productivity in Table 3) (Schmidt et al. 2017). I selected the variable that ranked highest when added to the top density dependent model from step one, then added all remaining environmental variables to that model again (excluding those directly related to a

chosen variable, such as the binary and non-binary measures of autumn harshness). I continued this iterative addition of remaining variables until the top model ceased to have an average ΔAICc of 2 points over the next best model, or additional variables ceased to improve model fit (see Appendix A for full model list).

2.4.2 Early Summer Density

I used a similar two-stage approach to assess the effects of weather variables on population patterns across winter seasons on all four plots. I calculated early summer estimates by plot/year in SECR and constructed bootstrapped datasets in the same way as described for the autumn dataset. I selected a slightly different set of environmental covariates (see Use in Table 3), excluding variables that would have impacted the population the previous summer in favor of only those impacting voles throughout the winter. I used exploratory plotting to assess the density dependent relationships, which prompted me to continue to include the autumn density estimate as a covariate, alongside a binary version of autumn density estimate with 10 voles per hectare serving as the cut off between high and low. The sine and cosine terms were also tested, to allow for multi-year patterns rather than only single year density dependence. I again ranked density dependent variables separately, then added environmental variables until additional variables ceased to improve model fit based on AICc. Inclusion of a random effect for year lead to singularity issues, so all early summer models were fit using the lm() function in the R stats package.

3. Results

3.1 Autumn Density

Between 1993 and 2022, a total of 3,428 individual northern red-backed voles were captured a collective 11,251 times across the four plots and two seasons. Animals varied in response to initial capture, with just over 41% being caught only once and others returning to traps on multiple occasions (Figure 4). For all four plots, the model including individual heterogeneity in capture probability (g_0) and variation in home range size (σ) by year was the

most parsimonious explanation of the data, with an AICc weight of 1 for all plots. Estimates for the post-hoc analysis were based on results from this model alone.

Red-backed vole density estimates for autumn displayed similar timing of highs and lows across plots, but with differing amplitudes (Figure 5). Density estimates varied dramatically during the sampling period, with autumn density estimates ranging from years with no detections at all (F2, 2004) to approximately 80 voles per hectare on F1 in 2017.

Only one plot (F1) exhibited a significant cyclical pattern based on post-hoc autocorrelation analysis (Figure 6). The three-year periodicity of the F1 plot is also evident in the phase plane diagram (Figure 7). A similar trend in autocorrelation was visible, but not significant, for F2, which registers as nearly cyclic with a three-year period on the phase diagram. Plot R1 showed little evidence of cyclicity, but R2 appeared to be weakly cyclic on the phase plane diagram (Figure 6, Figure 7).

The second stage of the autumn analysis, consisting of a model selection process to find patterns in amplitude, yielded a top model in which autumn density was a product of a sine wave with a period of 3, white spruce seeds, binary autumn harshness, and a random effect for year (mean $R^2_{marginal}$=0.36, mean ΔAICc 0.087, see Appendix A for full model selection table). Increased white spruce seed availability in a given autumn season led to higher vole density nearly a year later (α_{seeds} =0.50, 95% CI [0.20, 0.80]), whereas cold autumn temperatures led to decreased density in the following autumn ($\alpha_{ColdDaysB}$ =-0.63, 95% CI [-1.22, -0.04]). Although not included in the top model, there was also a noticeable correlation between autumn density and the number of rain-on-snow days (see Table 3 for variable explanation). The binary version of early season rain-on-snow days was the second best individual environmental predictor of amplitude after spruce seeds, and a simple linear model predicting autumn density using only this variable showed vole densities to be significantly lower after years with more than two days of rain before a foot of snow was established ($\alpha_{RainDaysB}$=-1.004, 95% CI [-1.447, -0.562]).

3.2 Early Summer Density

Early summer density estimates ranged between 0.3 and 5.8 voles per hectare, showing less pronounced extremes than those for autumn sessions due to minimal breeding time before sampling. Base models for this analysis included individual heterogeneity in capture probability, however due to a limited number of recaptures in spring I was unable to fit more complex models that included variation in home range size and instead used a simplified model that estimated a common home range size across years. I found a strong inverse trend between autumn densities and the following early summer, in which high autumn population densities were generally followed by lower early summer densities (Figure 8). For the post-hoc linear modeling, this relationship was best represented using a binary classification of autumn density as high or low, with 10 voles/ha serving as the threshold between categories (Appendix B).

White spruce seeds that fell the previous autumn were ranked highest against all other environmental variables, but did not show substantial improvement in fit over the density dependent model. Given the small sample size (n=36 plot years), addition of a random effect for year did not improve fit, leaving a top model where early summer density was best predicted by a binary representation of previous autumn density. A 95% confidence interval for the beta coefficient did not overlap zero (-0.97, 95% CI [-1.73, -0.20]), indicating that high autumn densities were typically followed by low early summers.

4. Discussion

Red-backed vole densities in this study exhibited tremendous variation, with populations ranging from no voles captured to levels higher than any reported in a 2012 review of North American trapping efforts for this species (Boonstra and Krebs 2012). However, no single trapping grid appeared to show consistently higher densities than others (Figure 5). Additionally, some peaks show fairly similar densities across trapping grids (such as in 2017), while others have a much more noticeable variability (2008 and 2014). This suggests that while some factors determining density can affect the plots equally, there are others that have more varied effects, despite being less than 400 m apart. These differences in density across plots could reflect

variation in vole productivity or survival, both of which can be tied to known habitat differences. I did not account for between-plot differences in snow depth, density, or structure in this study, although snow conditions could both directly and indirectly affect vole survival. Thorough snow surveys conducted during the last three years of this study showed that there can be a difference in snow depth of up to 15% between plots at peak snowfall, with the forest plots generally having deeper snowpacks than riparian areas. A study in Yukon Territories involving snow fences showed that lemmings and tundra voles preferred increased snow depth when selecting winter nest locations (Reid et al. 2012), a trend which could also apply to northern red-backed voles, who appear to form communal nests in the winter (West 1977). These differences in snow depth could also be especially impactful during shoulder seasons, when low depths in autumn or high density in spring cause snow to be less insulative. Although I did not explore the spring melt season in this study, it could serve as a similar bottleneck to vole survival as autumn snow establishment, particularly if animals are low on food resources after a long winter. Lastly, there could easily be differences in snow structure between plots; for example, the sparser tree cover and ridge location of forest plots could make wind crusts more common, whereas riparian plots could be more protected. This crust could decrease thermal protection for voles. Using recently collected snow data to assess plot level changes in snow characteristics could help illuminate reasons for variation in density between small mammal trapping grids.

Voles in the two habitats could also vary in their vulnerability to predators due to other factors, specifically due to differences in available escape. In addition to potential reduction in avian predation as a result of snow crust formation, a more dense undergrowth could provide protection from predation in the summer. The slight differences I observed in plant communities (forest plots have more shrub birch, while riparian plots have more graminoids) could also affect vole food availability such as berries, mushrooms, or other forbs. Although linking vole densities to berry and fungus availability has proven to be challenging (Krebs et al. 2010), I can reasonably assume that voles are dependent on consistent food sources and would choose their habitat accordingly.

My analyses suggest that these populations cycle on a somewhat less consistent period compared to earlier studies (Schmidt et al. 2017), likely due to a pair of two-year boom/bust

patterns between 2018 and 2022 (Figure 5). However, this irregularity in period should not be seen as a sign of the cyclic collapse similar to that in Europe, which has been characterized by substantial decreases in amplitudes (Ims et al. 2008, Cornulier et al. 2013). By contrast, my results show the opposite trend; with amplitudes of high years staying consistent or even increasing over time. This increase in amplitude seen during the mid-to late- 2000s and early 2010s has been previously explained by increases in primary productivity (Schmidt et al. 2017). Possible reasons for this discrepancy is that all four plots had previously been combined into a single density estimate by year whereas my study accounted for among plot differences in density, which may have masked the signal of NDVI. Additionally, the dynamics of the system may have changed in years since past analyses were conducted. Alternatively, this trend could be a product of a change in monitoring frequency that took place in 2003, in which trapping shifted from up to six one-week visits throughout the summer to a single visit in mid-August. Although early season incidental mortality is not recorded to be inordinately high, removing even a single breeding female from a population at the beginning of the summer could have substantial cascading effects. Northern red-backed voles have a gestation period of 19-23 days and display either post-partum estrous or an estrous cycle approximately 4-5 days after giving birth (Krebs and Wingate 1985). This means a breeding female could have up to 5 litters in a season, each containing approximately 6 pups who reach reproductive maturity in two months (Martell and Fuller 1979, Krebs and Wingate 1985). Early season young-of-the-year are thus capable of having up to two litters of their own during their birth summer (Martell and Fuller 1979). Given the coincidental timing of the shift in methodology, increases in primary productivity, and increase in vole amplitudes, an important direction for future study would be a more focused analysis of recent trends in primary productivity.

My data exhibited a periodicity that is less regular and more chaotic (sensu May, 1974), which could be a result of multiple factors. In the classic paper describing chaos in populations with non-overlapping generations, May (1974) describes a process in which a chaotic population may appear to have a three-year period bracketed by times with more erratic behavior given certain growth rates, which is similar to patterns I saw in my data (Figure 5). Although vole populations do overlap temporally, the mortality seen during the winter season is sufficiently high that parallels may still be drawn, and similar patterns may develop. Other studies have

suggested that predation by mustelids may lead to chaotic patterns, despite retaining a statistically significant periodic element (Hanski et al. 1993). Having data on mustelid predators could provide clarity in this regard for my own study, but in absence of that, continuation of long-term monitoring may shed light on the issue of periodicity.

Other important aspects of the trends in population density and cyclicity are the population differences between the forest and riparian habitats. The forest plots appeared to exhibit more cyclic fluctuations than the two riparian plots. In addition to the aforementioned differences in habitat, this could be a result of differing species dynamics. The riparian plots are also inhabited by tundra voles (*Microtus oeconomus*), who occasionally have equal or even greater population densities than northern red-backed voles. The presence of a separate prey species, which may respond to different environmental and density-related triggers, could create a system in which predators would prey-switch when their preferred species became less available. This would likely lead to weaker density-dependent cyclicity if the cycle was partially predator driven. Tundra voles are larger and generally more herbivorous (Baltensperger et al. 2015), primarily occupying the area of R2 that exhibits ephemeral streams and a more grassy habitat compared to the shrubby areas more commonly occurring elsewhere. This alternative habitat and potential for competition may also explain the generally lower population densities of northern red-backed voles on R2 (seen in Figure 5). A more in-depth assessment of the interspecific dynamics, including habitat preferences and density patterns of each vole species, could help shed light on this aspect.

One new finding from this study is the potential importance of white spruce mast, which has not been identified in past studies of northern red-backed voles (Krebs et al. 2010). Studies of vole stomach contents have indicated consumption of white spruce seeds and voles presented with them in lab trials readily eaten them, although they tended to lose weight if their diets consist entirely of spruce seeds (Grodzinski 1971). However, if spruce seeds were supplemented with lichen, animals maintained body weight, suggesting that they might be a helpful addition to overwinter food supply alongside more consistently available sources (Grodzinski 1971). This begs the question of whether the spruce seeds, which would become available in the autumn, are

acting as a food source on their own, or alternatively if the multi-annual patterns that trigger substantial spruce mast (see figure 2 in Roland et al. 2014) are separately affecting vole density.

Previous studies that have examined which weather patterns lead to spruce masting have found that weather events up to three years prior to seed fall can affect the magnitude of mast (Roland et al. 2014). Many of these events could also affect voles directly, such as low snow fall in the winter prior to seed fall and a cool, wet summer in the months leading up to seeds becoming available (Juday 2003, Roland et al. 2014). This chain of events could lead to low vole survival during the previous winter, continued lows during the summer due to slow growing conditions for other plants, and subsequently decreased likelihood of a density-dependent crash during the winter in which seeds were available. Weather events that increase spruce mast could also either positively or negatively affect production of other food sources, such as berries, which also appear to have multi-annual weather patterns leading up to high berry years (Krebs et al. 2009). Further exploration of vole diet would aid in determining the nature of the apparent relationship between voles and white spruce mast.

Understanding this link becomes especially important given changes anticipated for boreal ecosystems. As of summer 2022, an outbreak of spruce beetles (*Dendroctonus rufipennis*) which had previously been constrained to the southern Alaska Range, was found to have moved northward into the area of my study grid (Stehn and Syrotchen 2022). Although this type of infestation has been shown to have mixed effects on vole populations in other regions (McDonough and Rexstad 2005, Lance et al. 2006), we would expect the dramatic amplitude fluctuations over the past 10 years to dampen if voles are truly depending on spruce seeds as a food source.

The next most influential variable in the amplitude analysis was Cold Days, my metric of autumn harshness, which indicated that late snow onset coupled with cold weather led to low vole populations the following fall. Although these negative effects were occasionally overridden by other factors, such as when a harsh autumn coincided with a mast year in autumn of 2016, which in turn was followed by an extremely high vole population in 2017, this relationship should still signal a potential for concern, especially given predictions for progressively later

snow onset based on climate projections (Lader et al. 2020). Shortened snow seasons have been linked to cyclic collapse of voles in Europe (Ims et al. 2008), potentially due to shifts between specialist and generalist predation that usually accompany seasonal change (Tyson and Lutscher 2016). During summer, voles are vulnerable to predation by generalist predators such as foxes, or nomadic specialist predators (typically classified with generalists) such as small hawks and owls, and resident specialist predators, primarily weasels (Turchin and Hanski 1997). However, during the winter months, more predation pressure comes from specialists, which are considered to be the primary driver of cyclic patterns in vole densities seen throughout Europe (Hanski et al. 2001). Generalist predators have a tendency to stabilize cyclic relationships, adding a direct density dependent element rather than the delayed affect seen when a specialist predator grows as a response to high prey availability (Hanski et al. 1991). It follows that as the snow season grows shorter, leaving a longer time of year in which voles are subjected to generalist predators, cyclicity may eventually give way to a lower stable equilibrium (Tyson and Lutscher 2016). Coupled with the predictions for decreased snow season length as a result of climate change (Lader et al. 2020), this mechanism suggests the potential for a tipping point that could cause dramatic changes to small mammal populations.

Similarly, rain-on-snow events could become a prominent factor affecting winter population dynamics because of climate change. Although this variable was not in my top model, preliminary examination of autumn densities and early-snow-season rain-on-snow days showed a limiting relationship, in which high rain-on-snow occurrences prevented densities the following year from spiking. This aligns with the findings of other studies (Soininen et al. 2015, Fauteux et al. 2021) and can be explained by the potential for higher density snow near the base of the snowpack, with the accompanying effects on mobility, food availability, and decreased insulative value. The lack of inclusion in the final model could be a result of how the variable itself was calculated; future studies may want to account for duration or severity of rain events. The timing of such events could be crucial, as ice crusts higher in the snowpack, such as those observed in the winter of 2021-2022, may serve as a helpful barrier to plunging predators, however they may also hamper vole's ability to escape, making them more vulnerable to predators while on the surface (Berteaux et al. 2017). Later season rain-on-snow events were not examined, but could

prove helpful for predicting patterns in vole density resulting from more stochastic winter weather.

My only significant result of the early summer density analysis was the inverse relationship between density in autumn and the following spring. Both extremes are illustrated by F1, which showed both an uncharacteristically low autumn density of less than 2 voles/ha (2020) followed by a spring with around 10 voles/ha, and an extreme high of over 50 voles/ha (autumn 2021) followed by crash to less than 2 voles/ha the next spring (2022). Although voles are likely not reproductive during the winter (Stevenson et al. 2009), my sampling timing was such that first litter born to overwintered animals was out of the nest, causing the apparent increases over winter months. Almost no years with elevated densities in the autumn remained high, but not all years with low autumn population were followed by high early summer densities, likely a product of the many other environmental or internal factors that could limit populations from spiking. This suggests a sort of density dependence, but with an unknown cause. Increased mortality after a peak could be a result of food shortage over the winter months due to the population being at or near carrying capacity, similar to patterns found in field voles (*Microtus agrestis*) (Huitu et al. 2003) and bank voles (*Myodes glareolus*) (Johnsen et al. 2017). However, it could also represent a predator response, wherein a specialist predator such as short-tailed weasels show a strong but slightly delayed population increase in reaction to heightened prey availability. Mustelids may not reproduce in times of insufficient prey (Erlinge 1974) and have longer generation times when they are reproductive, causing them to increase more slowly than voles. This lag would result in the effects of predation not being immediately apparent during the summer in which vole populations were rapidly increasing, but rather over the following winter when weasel populations had increased and voles were no longer reproducing. This is another question that would be more easily answered with additional data on predation and diet, which I recommend for further study. Lastly, this result differs from our observations from the full autumn dataset in that overwinter weather effects like fall harshness do not appear to be influential. This is likely a product of small sample size, but could also be due to the years for which spring data is available. Most paired autumn/spring data was collected in the 1990s, when fall harshness was generally lower and may have been less impactful. Continued monitoring of spring vole populations under current climate conditions could combat both issues,

potentially providing high enough sample size for more complex models and increasing the chances of capturing changing climate effects.

5. Conclusions

During the last three decades, the vole populations at the study site in Denali National Park and Preserve have shown cyclicity, but with some variation in both period and amplitude. Winter continues to be a highly influential time, often incurring the crash phase after a population high. My ability to model density dependent relationships and their interactions with environmental factors highlights the importance of both long-term monitoring and co-located studies, as we, for example, benefitted greatly from nearby sources of weather and seed fall data. Surprisingly, snow conditions do not appear to exert as strong of an impact on red-backed vole populations in Denali as shown elsewhere, possibly because we have not yet reached important climate thresholds with regard to snow season length, or duration and severity of stochastic weather events. Continued monitoring of snow characteristics will be vital in this effort. Including research on vole predators could illuminate many of the existing uncertainties highlighted by this study, including the mechanism of winter declines and cyclicity. This could also help discern the potential ramifications of changes in snow season, and assess how alterations in vole populations over time could affect higher trophic levels within interior Alaska. As a short-lived mammals with high reproductive rates and more rapid population cycles, red-backed vole populations may show changes before they impact their many predators, and can serve as an early warning sign of a changing ecosystem. I recommend their continued study and further efforts to understand their interactions with other vole species, predators, and diet patterns in Interior Alaska.

References

Baltensperger, A. P. et al. 2015. Quantifying trophic niche spaces of small mammals using stable isotopes (δ15N and δ13C) at two scales across Alaska. - Can. J. Zool. 93: 579–588.

Berteaux, D. et al. 2017. Effects of changing permafrost and snow conditions on tundra wildlife: critical places and times. - Arct. Sci. 3: 65–90.

Bilodeau, F. et al. 2013. The effect of snow cover on lemming population cycles in the Canadian High Arctic. - Oecologia 172: 1007–1016.

Bjornstad, O. N. et al. 1995. A geographic gradient in small rodent density fluctuations: a statistical modelling approach. - Proc. R. Soc. B Biol. Sci. 262: 127–133.

Bogdziewicz, M. et al. 2016. Negative effects of density on space use of small mammals differ with the phase of the masting-induced population cycle. - Ecol. Evol. 6: 8423–8430.

Boonstra, R. and Krebs, C. J. 2012. Population dynamics of red-backed voles (Myodes) in North America. - Oecologia 168: 601–620.

Boonstra, R. et al. 1998a. Population cycles in small mammals: the problem of explaining the low phase. - Ecology 79: 1479–1488.

Boonstra, R. et al. 1998b. The impact of predator-induced stress on the snowshoe hare cycle. - Ecol. Monogr. 68: 371–394.

Burnham, K. P. and Anderson, D. R. 2002. Model Selection and Multimodel Inference: A Practical Information-Theorhetical Approach. - Springer-Verlag.

Cornulier, T. et al. 2013. Europe-wide dampening of population cycles in keystone herbivores. - Science 340: 63–66.

Domine, F. et al. 2018. Snow physical properties may be a significant determinant of lemming population dynamics in the high Arctic. - Arct. Sci. 4: 813–826.

Duchesne, D. et al. 2011. Habitat selection, reproduction and predation of wintering lemmings in the Arctic. - Oecologia 167: 967–980.

Efford, M. 2020. secr 4 . 2 - spatially explicit capture – recapture in R.

Efford, M. G. and Fewster, R. M. 2013. Estimating population size by spatially explicit capture-recapture. - Oikos 122: 918–928.

Elias, S. P. et al. 2006. A Cyclic Red-Backed Vole (Clethrionomys Gapperi) Population and Seedfall Over 22 Years in Maine. - J. Mammal. 87: 440–445.

Erlinge, S. 1974. Distribution, Territoriality and Numbers of the Weasel Mustela nivalis in Relation to Prey Abundance. - Oikos 25: 308–314.

Falls, J. B. et al. 2007. Fluctuations of deer mice in Ontario in relation to seed crops. - Ecol. Monogr. 77: 19–32.

Fauteux, D. et al. 2015. Cyclic Dynamics of a Boreal Southern Red-Backed Vole Population in Northwestern Quebec. - J. Mammal. 96: 573–578.

Fauteux, D. et al. 2021. Climate variability and density-dependent population dynamics: Lessons from a simple high-Arctic ecosystem. - PNAS 118: 1–7.

Flamme, M. J. et al. 2018. Small Mammal Monitoring Protocol for the Central Alaska Network.

Gilg, O. et al. 2003. Cyclic Dynamics in a Simple Vertebrate Predator-Prey Community. - Science (80-.). 302: 866–868.

Gilg, O. et al. 2009. Climate change and cyclic predator-prey population dynamics in the high Arctic. - Glob. Chang. Biol. 15: 2634–2652.

Ginzburg, L. R. and Krebs, C. J. 2015. Mammalian cycles: Internally defined periods and interaction-driven amplitudes. - PeerJ 2015: 2–10.

Grodzinski, W. 1971. Energy Flow Through Populations of Small Mammals in the Alaskan Taiga Forest. - Bialowieza 16: 231–275.

Hanski, I. et al. 1991. Specialist Predators , Generalist Predators , and the Microtine Rodent Cycle. - J. Anim. Ecol. 60: 353–367.

Hanski, I. et al. 1993. Population oscillations of boreal rodents: regulation by mustelid predators leads to chaos. - Lett. to Nat. 364: 232–235.

Hanski, I. et al. 2001. Small-rodent dynamics and predation. - Ecology 82: 1505–1520.

Huitu, O. et al. 2003. Winter food supply limits growth of northern vole populations in the absence of predation. - Ecology 84: 2108–2118.

Ims, R. A. and Fuglei, E. 2005. Trophic Interaction Cycles in Tundra Ecosystems and the Impact of Climate Change. - Bioscience 55: 311.

Ims, R. A. et al. 2008. Collapsing population cycles. - Trends Ecol. Evol. 23: 79–86.

Johnsen, K. et al. 2017. Surviving winter: Food, but not habitat structure, prevents crashes in cyclic vole populations. - Ecol. Evol. 7: 115–124.

Juday, G. P. 2003. A 200-year perspective of climate variability and the response of white spruce in interior Alaska. - In: Greenland, D. et al. (eds), Climate Variability and Ecosystem Response at Long-Term Ecological Research Sites. Oxford University Press (OUP), pp. 226–250.

Klemola, T. et al. 2002. Specialist and generalist natural enemies as an explanation for geographical gradients in population cycles of northern herbivores. - Oikos 99: 83–94.

Korpela, K. et al. 2013. Nonlinear effects of climate on boreal rodent dynamics: Mild winters do not negate high-amplitude cycles. - Glob. Chang. Biol. 19: 697–710.

Korpimäki, E. et al. 2002. Dynamic effects of predators on cyclic voles: Field experimentation and model extrapolation. - Proc. R. Soc. B Biol. Sci. 269: 991–997.

Korslund, L. and Steen, H. 2006. Small rodent winter survival: Snow conditions limit access to food resources. - J. Anim. Ecol. 75: 156–166.

Krebs, C. J. and Myers, J. H. 1974. Population Cycles in Small Mammals. - Adv. Ecol. Res. 8: 267–399.

Krebs, C. J. and Wingate, I. 1985. Population Fluctuations in the Small Mammals of the Kluane Region, Yukon Territory. - Can. Field-Naturalist 99: 51–61.

Krebs, C. J. et al. 2009. Climatic determinants of berry crops in the boreal forest of the southwestern Yukon. - Botany 87: 401–408.

Krebs, C. J. et al. 2010. Do changes in berry crops drive population fluctuations in small rodents in the southwestern Yukon? - J. Mammal. 91: 500–509.

Lader, R. et al. 2020. Anticipated changes to the snow season in Alaska: Elevation dependency, timing and extremes. - Int. J. Climatol. 40: 169–187.

Lance, E. W. et al. 2006. Spruce beetles and timber harvest in Alaska: Implications for northern red-backed voles. - For. Ecol. Manage. 222: 476–479.

Lindström, E. R. and Hörnfeldt, B. 1994. Vole Cycles, Snow Depth and Fox Predation. - Oikos 70: 156.

Littell, J. S. et al. 2018. Alaska snowpack response to climate change: Statewide snowfall equivalent and snowpack water scenarios. - Water 10: 1–16.

Maccluskie, M. and Oakley, K. 2003. Central Alaska Netweork Vital Signs Monitoring Plan.

Martell, A. M. and Fuller, W. A. 1979. Comparative demography of Clethrionomys rutilus in taiga and tundra in the low Arctic. - Can. J. Zool. 57: 2106–2120.

McDonough, T. J. and Rexstad, E. 2005. Short-Term Demographic Response of the Red-Backed. - J. Wildl. Manage. 69: 246–254.

Mihok, S. et al. 2019. The Characterization of Vole Population Dynamics. - Ecol. Monogr. 55: 399–420.

Oakley, K. L. and Boudreau, S. L. 2000. Conceptual Design of the Long-term Ecological Monitoring Program for Denali National Park and Preserve.

Overland, J. et al. 2019. The urgency of Arctic change. - Polar Sci. 21: 6–13.

Penczykowski, R. M. et al. 2017. Winter is changing: Trophic interactions under altered snow regimes. - Food Webs 13: 80–91.

Reid, D. G. et al. 2012. Lemming winter habitat choice: A snow-fencing experiment. - Oecologia 168: 935–946.

Rennert, K. J. et al. 2009. Soil thermal and ecological impacts of rain on snow events in the circumpolar arctic. - J. Clim. 22: 2302–2315.

Roland, C. A. et al. 2004. Monitoring vegetation structure and composition at multiple spatial scales in the Central Alaska Network.: 1–50.

Roland, C. A. et al. 2014. Climate sensitivity of reproduction in a mast-seeding boreal conifer across its distributional range from lowland to treeline forests. - Oecologia 174: 665–677.

Royama, T. 1992. Analytical population dynamics. - Chapman and Hall.

Royle, J. A. et al. 2014. Chapter 5 - Fully Spatial Capture-Recapture Models. - In: Spatial Capture-Recapture. Academic Press, pp. 127.

Schmidt, J. H. et al. 2017. Weather-driven change in primary productivity explains variation in the amplitude of two herbivore population cycles in a boreal system. - Oecologia 186: 435–446.

Soininen, E. M. et al. 2015. Under the snow: a new camera trap opens the white box of subnivean ecology. - Remote Sens. Ecol. Conserv. 1: 29–38.

Sousanes, P. J. and Hill, K. R. 2015. Annual Climate Summary 2013 Central Alaska Network. - Nat. Resour. Data Ser.

Sousanes, P. and Hill, K. 2018. Weather & Climate Summary.

Stehn, S. Personal Communication. January 2023.

Stehn, S. and Syrotchen, J. 2022. Assessing the Risk of Denali's Forests to Spruce Beetle Outbreak.

Stenseth, N. C. 1999. Population Cycles in Voles and Lemmings: Density Dependence and Phase Dependence in a Stochastic World. - Oikos 87: 427–461.

Stevenson, K. T. et al. 2009. The seasonality of reproduction in photoperiod responsive and nonresponsive northern red-backed voles (Myodes rutilus) in Alaska. - Can. J. Zool. 87: 152–164.

Sundell, J. et al. 2019. Do phase-dependent life history traits in cyclic voles persist in a common environment? - Oecologia 190: 399–410.

Terraube, J. et al. 2015. Coping with fast climate change in northern ecosystems: Mechanisms underlying the population-level response of a specialist avian predator. - Ecography (Cop.). 38: 690–699.

Turchin, P. and Hanski, I. 1997. An Empirically Based Model for Latitudinal Gradient in Vole Population Dynamics. - Am. Nat. 149: 842–874.

Tyson, R. and Lutscher, F. 2016. Seasonally varying predation behavior and climate shifts are predicted to affect predator-prey cycles. - Am. Nat. 188: 539–553.

West, S. D. 1977. Midwinter aggregation in the northern red-backed vole, Clethrionomys rutilus. - Can. J. Zool. 55: 1404–1409.

Table 1. Mean percent cover estimates by vegetation type. Berry producing shrubs were classified separately to other shrubs to reflect potential small mammal food sources. Percent cover estimates were calculated from 12 vegetation monitoring sites, 3 located in each small mammal trapping grid.

Life Form	Forest	Riparian
moss	68.9	73.5
shrub	47.7	42.6
berry	41.2	35.2
graminoid	21.8	9.4
tree	11.6	10.6
forb	4.5	8.7
lichen	4.0	2.8

Table 2. Plot center coordinates and years of use for the four plots used for this study.

Plot	Center Latitude	Center Longitude	Elevation	Years Used
Riparian 1	63.731	-148.984	739 m	June: 1993, 1997-2002, 2020-2022 August: 1993, 1997-2022
Riparian 2	63.730	-148.981	724 m	June: 1993-2002, 2020-2022 August: 1993-2022
Forest 1	63.729	-148.989	776 m	June: 1993-2002, 2020-2022 August: 1993-2018, 2020-2022
Forest 2	63.727	-148.981	752 m	June: 1997-1999, 2002, 2020-2022 August: 1997-2018, 2020-2022

Table 3. Complete list of variables used for linear models. Use category specifies whether a variable was used to model differences in density between autumn and the following early summer (S) or in autumn only models (A)

Variable Name	Use	Description
Environmental Variables		
AddSnowDepth	S, A	Additive snow depth calculated throughout the snow year
MnSnowDepth	S, A	Mean snow depth, calculated as additive snow depth/days in snow year
MeltDays	S, A	Number of days between snow on date and establishment of at least 30cm of snow during which mean temperature exceeded 0°C
MeltDaysB	S, A	Binary version of MeltDays to represent threshold of 5 days of melt prior to establishment of >30cm of snow

Table 3 Contd.

Variable Name	Use	Description
RainDays	S, A	Number of days between snow on date and establishment of at least 30cm of snow during which mean temperature exceeded 0°C and precipitation was recorded
RainDaysB	S, A	Binary version of RainDays to represent threshold of 2 days of rain during prior to establishment of >30cm of snow
ColdDays	S, A	Number of days, beginning in August, Aor which minimum temperature was below -17°C and snow depth had yet to exceed the thermal threshold of 20 cm
ColdDaysB	S, A	Binary version of ColdDays to represent a threshold of 5 cold days prior to establishment of >20cm of snow
SeasonLength	S, A	Number of days in a given snow season relative to the average snow season found during the study period
SpringPrecip	S, A	Cumulative precipitation falling in April and May
SummerPrecip	A	Cumulative precipitation falling between snow off and August 1st
PrevSummerPrecip	A	Cumulative precipitation falling between snow off and snow on during the previous summer
GDD	A	Growing degree days, metric of plant growth potential when average temperature exceeds 5°C through August 1st
GDDPrev	A	Growing degree days, metric of plant growth potential when average temperature exceeds 5°C throughout the previous summer
Productivity	A	Combination of 3-year retrogressive averages of mean snow depth, cumulative summer precipitation, and growing degree days to represent multi-year increased primary productivity
Seeds	S, A	White spruce (Picea glauca) seed fall, measured in mean seeds captured in seed traps (See Roland et al. 2014 for protocol)
	Density Dependent Variables	
PrevHiLo	S, A	Binary expression of autumn density estimate from the previous year, with 10 voles/ha as the threshold distinguishing high from low

Table 3 Contd.

Variable Name	Use	Description
AutumnEst	S, A	Bootstrapped distribution of densities from autumn of the previous year, constructed using the mean and standard error of the top-ranking model for each plot
Cosine	S, A	Cosine wave with two- or three-year period
Sine	S, A	Sine wave with three-year period (two-year period resulted in zero values)

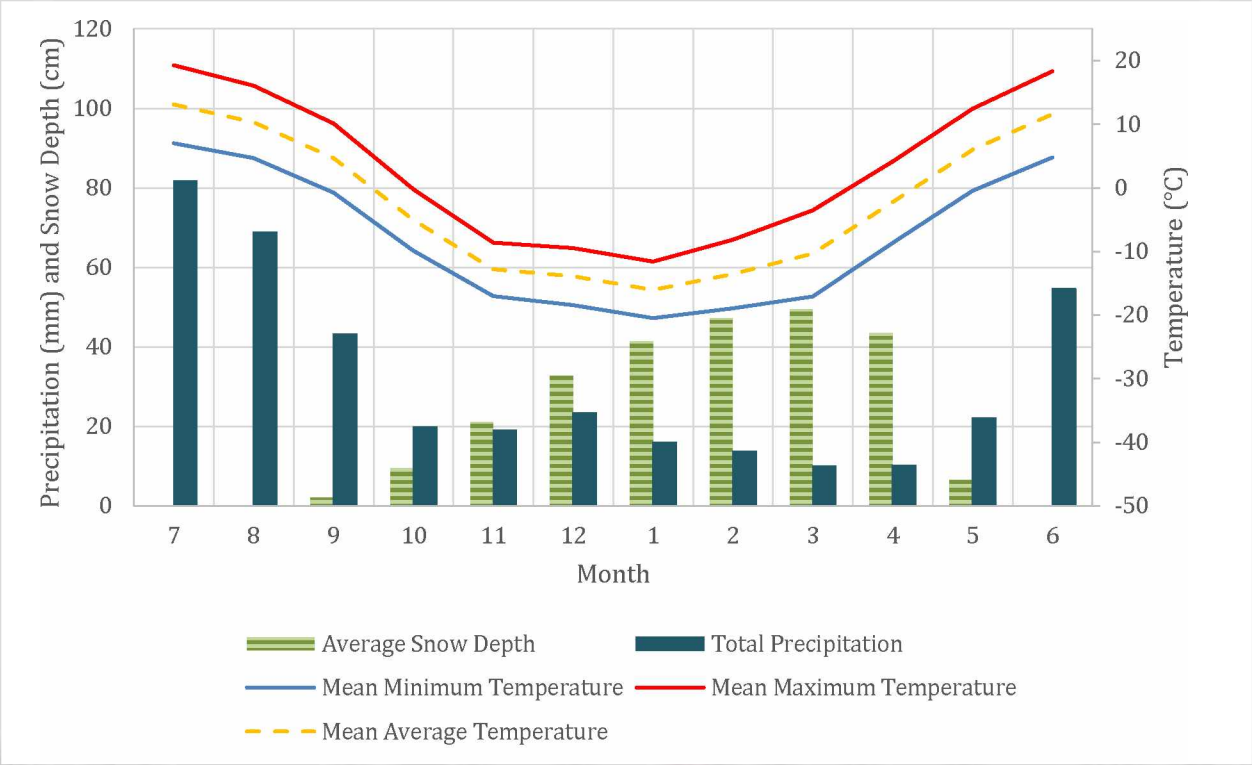

Figure 1. Temperature and precipitation trends recorded at the weather station near the Denali National Park and Preserve Headquarters, Alaska, located approximately1.6 km from the Rock Creek study site. This graph is arranged from July to the following June to place emphasis on winter months. Total precipitation is given in mm, whereas Average Snow Depth is given in cm. Values are based on means of measurements taken between 1981 and 2010.

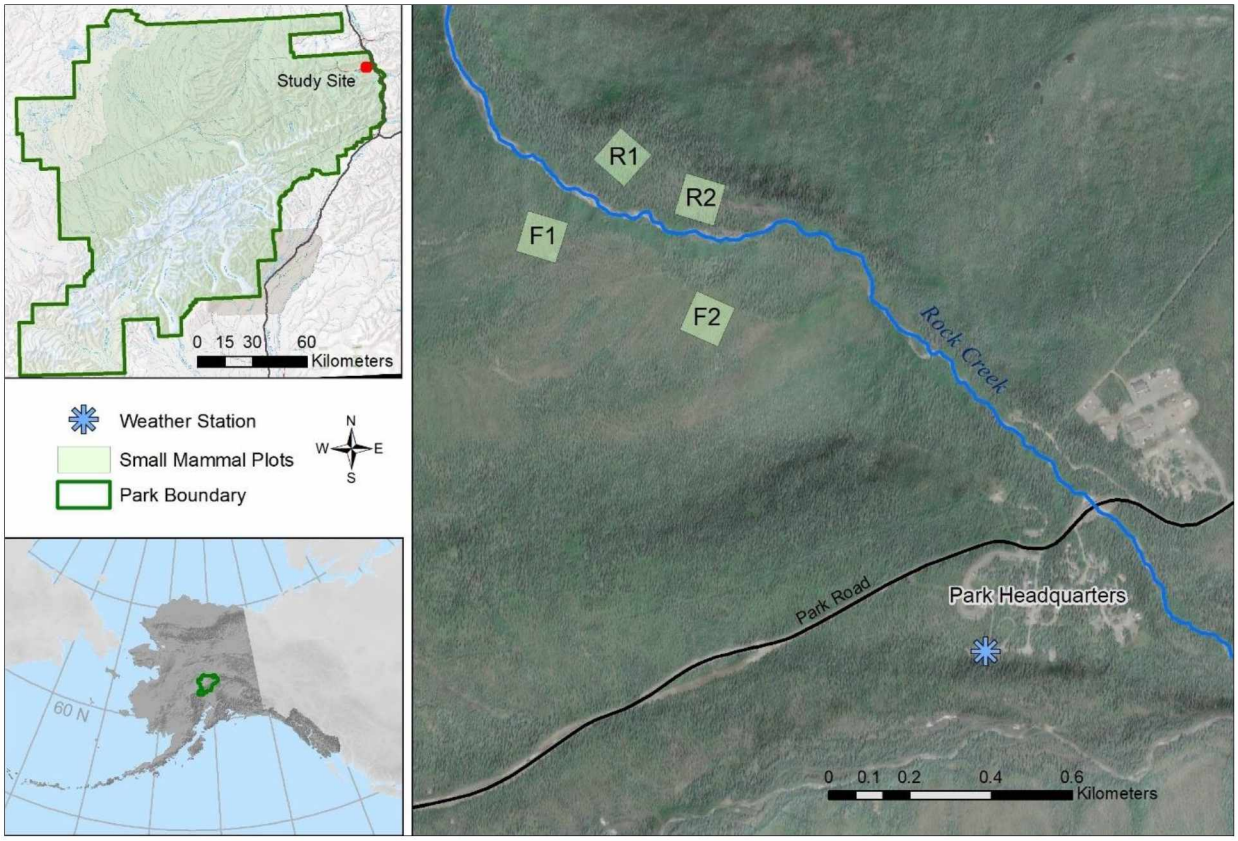

Figure 2. Location of the small mammal monitoring plots in Denali National Park and Preserve. Forest and riparian grids are located on opposite sides of Rock Creek (shown by the blue line). The weather station is marked with the blue asterisk.

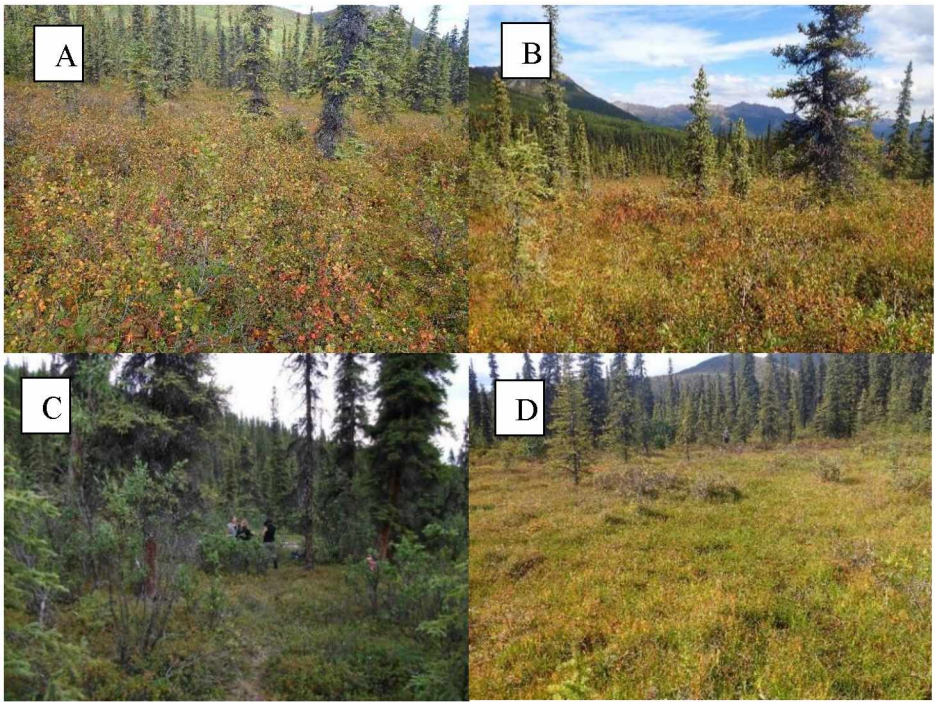

Figure 3. Photographs showing vegetation and structure of the four plots included in this study. A) Forest 1 (F1) B) Forest 2 (F2) C) Riparian 1 (R1). D) Meadow on bottom half of Riparian 2 (R2).

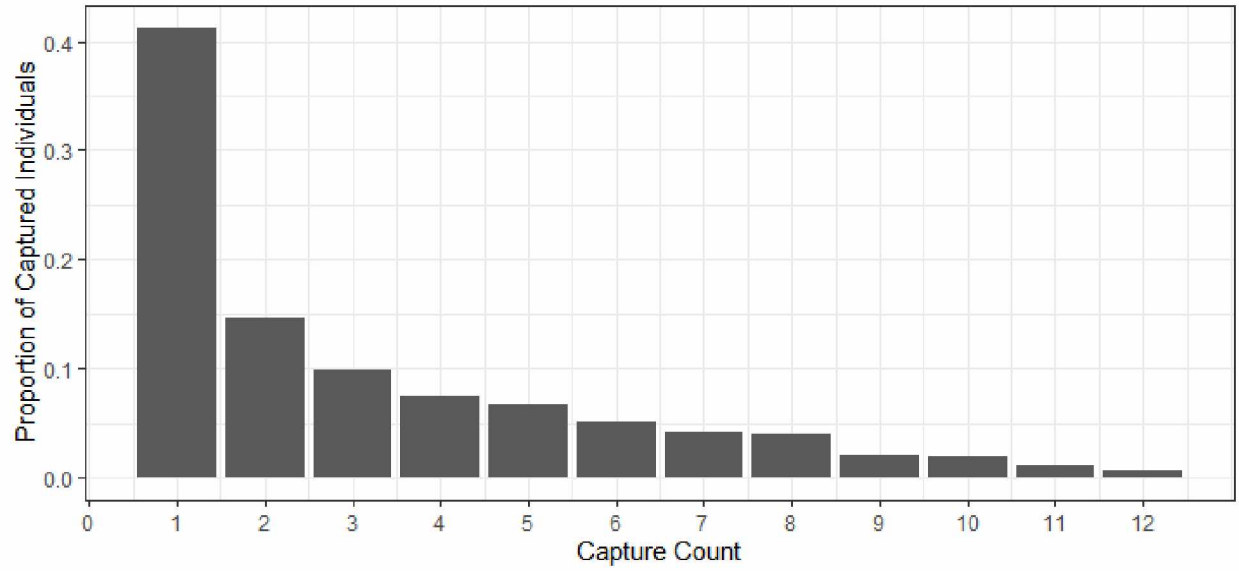

Figure 4. Capture summary for all individual voles captured across trapping grids and seasons 1993-2022.

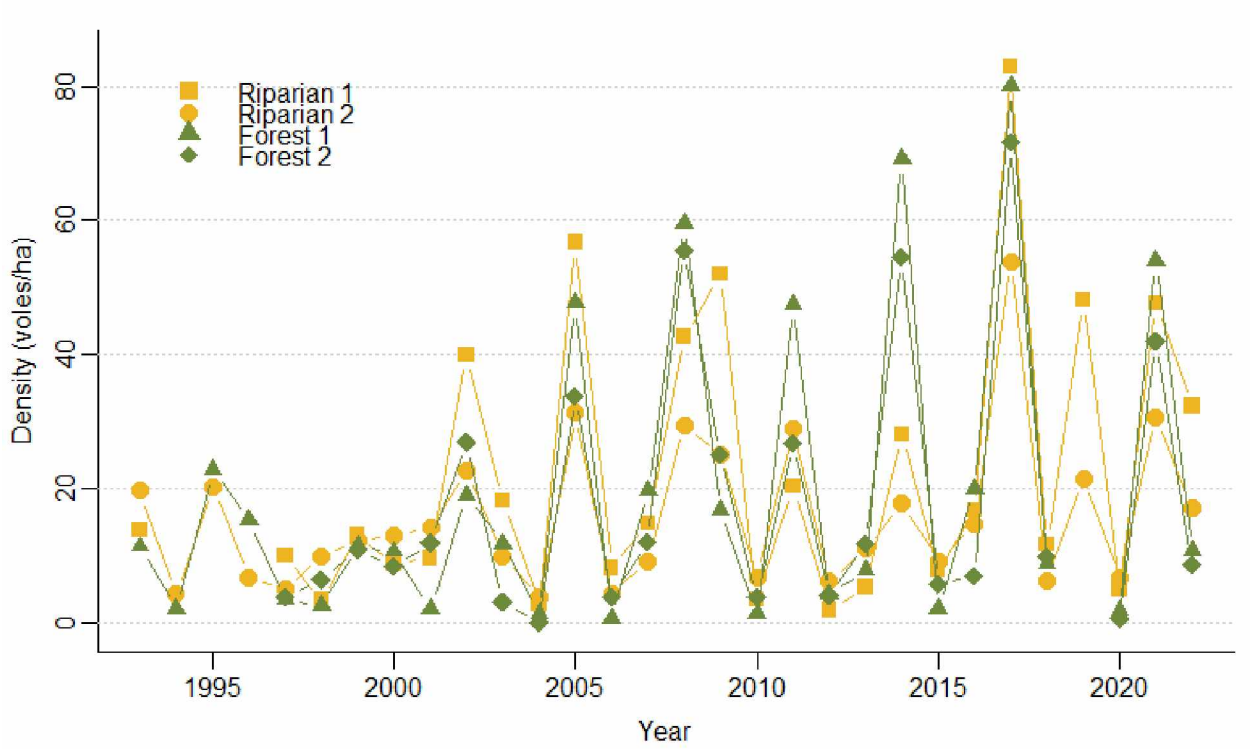

Figure 5. Autumn density estimates (voles/hectare) for northern red-backed voles on four plots in the Rock Creek watershed of Denali National Park and Preserve. All plots were 100 m^2, included 100 traps, and were monitored for four days during the second week of August.

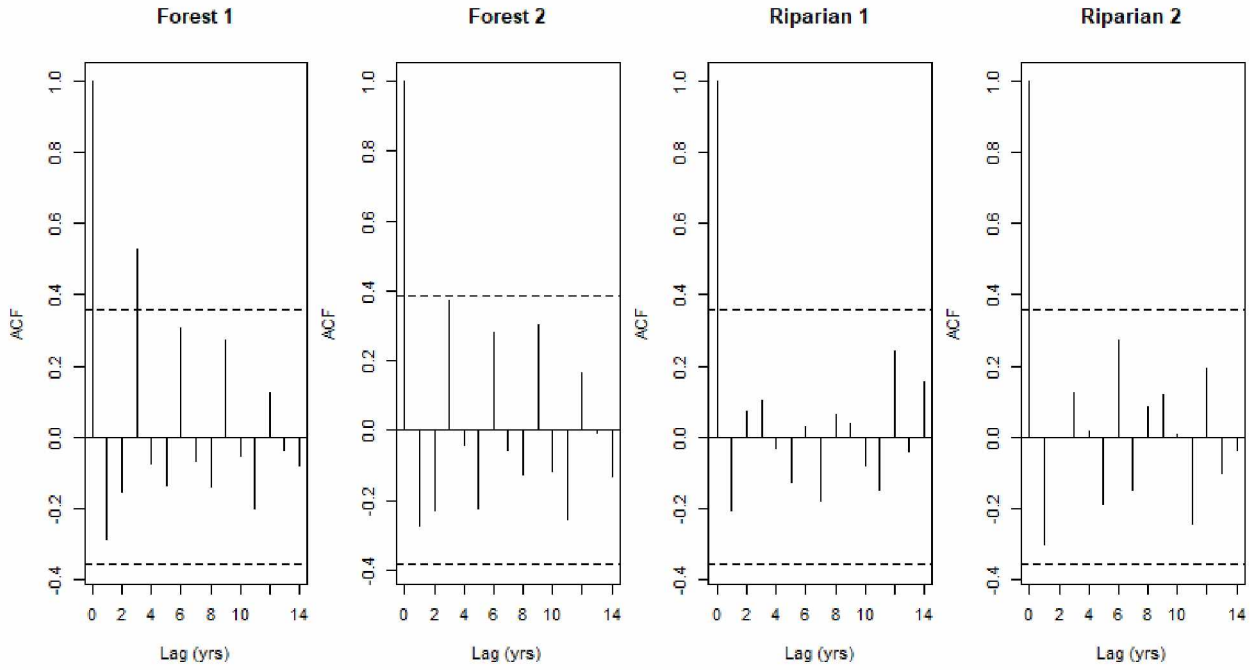

Figure 6. Autocorrelation plots (ACF = autocorrelation function) for vole density estimates found on each of the four plots in the Rock Creek watershed of Denali National Park and Preserve. Dotted lines represent a 95% confidence interval, and lines that extend beyond this interval represent significant autocorrelation (cyclicity) for a given number of years.

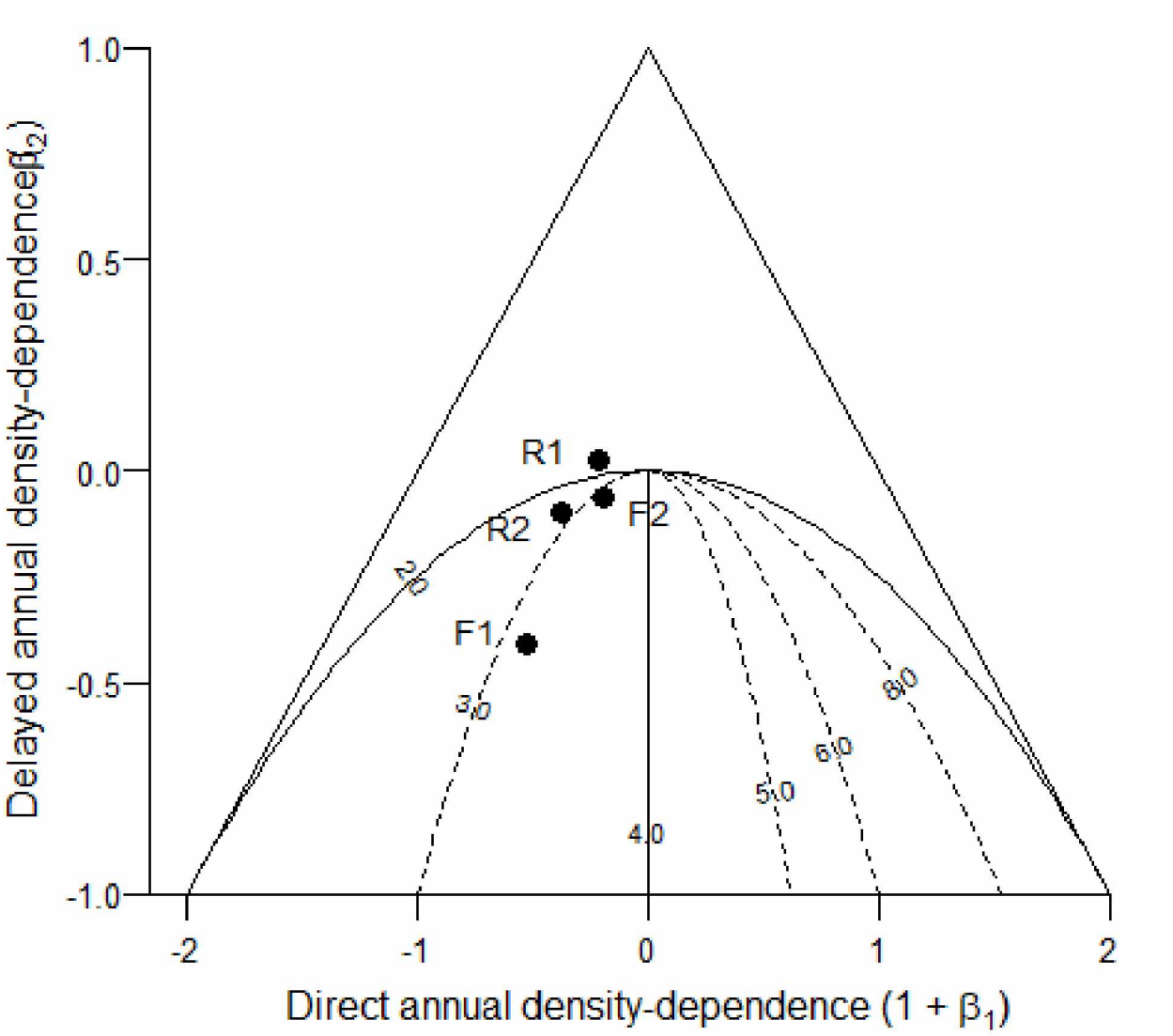

Figure 7. Phase plane diagram displaying estimated strengths of direct and delayed density dependence for four plots in the Rock Creek watershed. Values represent beta coefficients from a log-linear autoregressive model ($x_t = \beta_0 + (1 + \beta_1)x_{t-1} + \beta_2 x_{t-2}$) over the 30-year time series from 1993-2022. Points falling above the semicircle represent a lack of density-dependence, while those falling within the semicircle represent cyclicity on a period specified by section. Values of the dotted lines correspond to the cyclicity (in years) identified by the model. The triangle signifies the range of possible values of beta coefficient combinations for which populations are sustained over time (Stenseth 1999). Period strength increases through a decrease in delayed density-dependence (β_2) while period length increases with higher direct density-dependence $(1 + \beta_1)$ if the corresponding delayed coefficient is in the cyclic region.

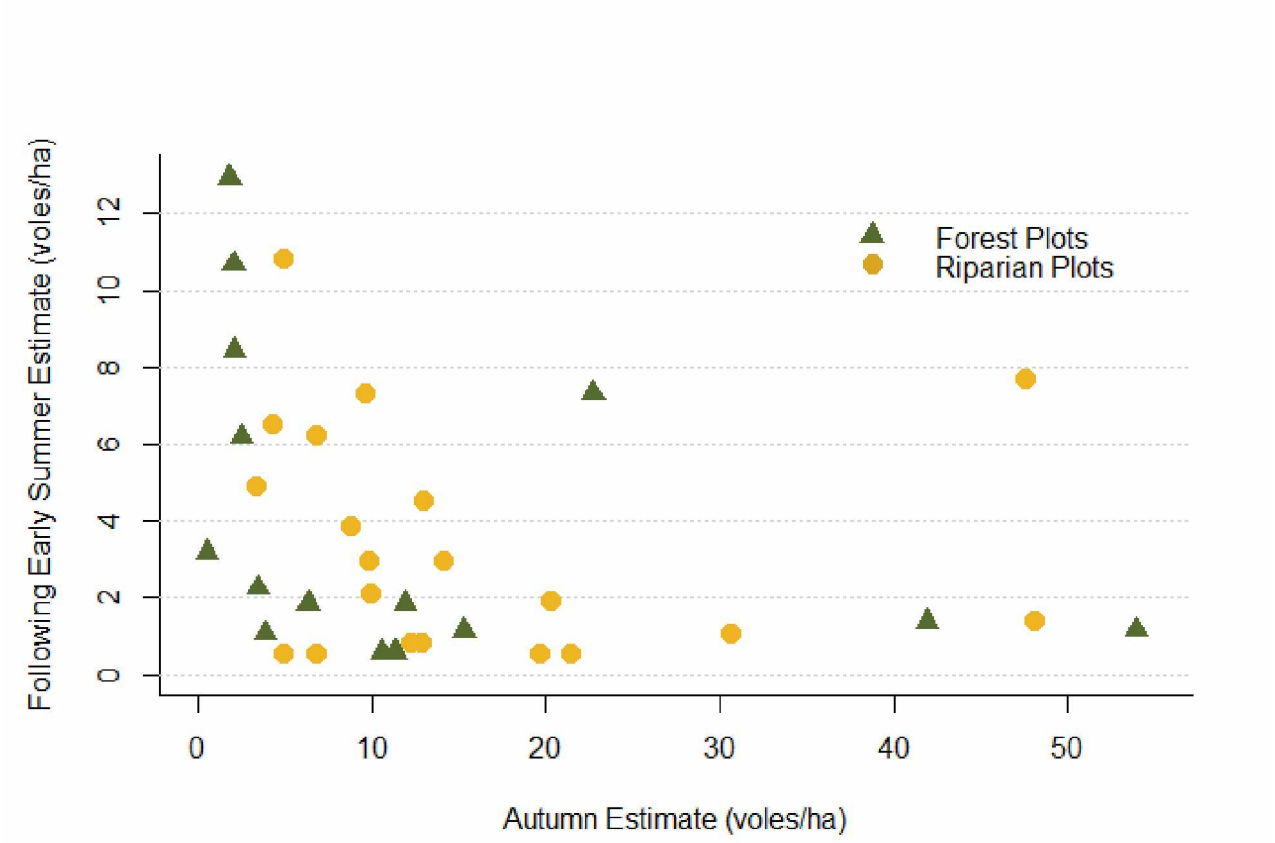

Figure 8. Northern red-backed vole density estimates for the autumn and following spring, measured between 1992-2002 in Denali National Park and Preserve, Alaska. All autumn estimates were taken from sampling that occurred during the second week of August, while early summer estimates for most years came from the third week of June. Early summer estimates were taken after the first litter was born, causing some years to show higher densities in early summer than had been present in autumn.

Appendices

Appendix A. Model ranking structure for fall amplitude analysis.

	Model	Mean Rank	Rank SD	Mean Wt	Wt SD	Mean ΔAIC	ΔAIC SD
Density Dependent (DD) Variables							
1	Dt ~ sine3 + (1|Year)	1.122	0.3595	0.3602	0.0903	0.0679	0.2678
2	Dt ~ cos2 + (1|Year)	2.676	1.2404	0.1641	0.0723	1.7784	1.2438
3	Dt ~ cos3 + sine3 + (1|Year)	3.38	1.2341	0.1191	0.0293	2.2756	0.4258
4	Dt ~ 1 + (1|Year)	4.048	1.0053	0.0998	0.0258	2.6371	0.8298
5	Dt ~ PrevHiLo + (1|Year)	4.912	1.7763	0.0852	0.0582	3.2421	1.4213
6	Dt ~ Dt-1 + sine3 + (1|Year)	5.719	1.4100	0.0563	0.0313	3.9533	1.0572
7	Dt ~ cos3 + (1|Year)	7.417	1.4857	0.0331	0.0109	4.8802	0.9739
8	Dt ~ Dt-1 + (1|Year)	8.539	1.2618	0.0249	0.0193	5.7573	1.5593
9	Dt ~ Dt-1 + cos2 + (1|Year)	8.577	1.2968	0.0241	0.0151	5.7332	1.5183
10	Dt ~ Dt-1 + cos3 + sine3 + (1|Year)	8.74	1.3536	0.0226	0.0150	5.8601	1.2685
11	Dt ~ Dt-1 + cos3 + (1|Year)	10.87	0.5073	0.0104	0.0097	7.6633	1.7975
Environmental Variable Models							
1	Dt ~ sine3 + seedscale + ColdDaysJB + (1|Year))	1.233	0.5301	0.1470	0.0314	0.0872	0.2437
2	Dt ~ sine3 + seedscale + ColdDaysJB + RainDaysB + (1|Year))	3.05	1.4005	0.0891	0.0350	1.1834	0.6538
3	Dt ~ sine3 + seedscale + (1|Year))	3.206	1.8759	0.0831	0.0255	1.2847	0.9405
4	Dt ~ sine3 + seedscale + RainDaysB + (1|Year))	4.251	2.1087	0.0680	0.0230	1.6936	0.9206
5	Dt ~ sine3 + seedscale + ColdDaysJB + MeltDaysB + (1|Year))	5.225	1.8493	0.0522	0.0158	2.1929	0.5092
6	Dt ~ sine3 + seedscale + ColdDaysJB + SumPrecipPrevS + (1|Year))	7.938	2.8316	0.0371	0.0117	2.8804	0.6178
7	Dt ~ sine3 + seedscale + SumPrecipPrevS + (1|Year))	9.202	4.4939	0.0368	0.0158	2.9842	1.1242
8	Dt ~ sine3 + seedscale + ColdDaysJB + RainDays + (1|Year))	9.284	4.5942	0.0347	0.0129	3.0524	0.6030

9	Dt ~ sine3 + seedscale + ColdDaysJB + AvgDepthS + (1|Year))	9.672	2.8363	0.0291	0.0069	3.3352	0.3669
10	Dt ~ sine3 + seedscale + MeltDaysB + (1|Year))	10.823	4.9736	0.0312	0.0136	3.3177	1.1050
11	Dt ~ sine3 + seedscale + ColdDaysJB + IntSnowDepthS + (1|Year))	11.433	3.0563	0.0269	0.0059	3.4847	0.3264
12	Dt ~ sine3 + seedscale + ColdDaysJB + LengthS + (1|Year))	13.583	4.6459	0.0247	0.0067	3.6771	0.3908
13	Dt ~ sine3 + seedscale + ColdDaysJB + SumPrecipS + (1|Year))	13.716	4.2755	0.0239	0.0062	3.7329	0.3806
14	Dt ~ sine3 + seedscale + ColdDaysJB + SprPrecipS + (1|Year))	15.471	3.9351	0.0215	0.0044	3.9298	0.2645
15	Dt ~ sine3 + RainDaysB + (1|Year))	16.072	7.5274	0.0228	0.0107	3.9850	1.1774
16	Dt ~ sine3 + seedscale + ColdDaysJB + GDDPrevS + (1|Year))	17.71	4.3378	0.0199	0.0040	4.0832	0.2692
17	Dt ~ sine3 + seedscale + RainDays + (1|Year))	18.147	4.3304	0.0172	0.0047	4.4110	0.8889
18	Dt ~ sine3 + seedscale + ColdDaysJB + MeltDays + (1|Year))	18.472	4.5008	0.0195	0.0040	4.1193	0.2752
19	Dt ~ sine3 + seedscale + ColdDaysJB + GDDS + (1|Year))	19.66	4.6802	0.0189	0.0039	4.1872	0.2683
20	Dt ~ sine3 + seedscale + SprPrecipS + (1|Year))	20.317	3.7022	0.0150	0.0039	4.6733	0.8225
21	Dt ~ sine3 + seedscale + IntSnowDepthS + (1|Year))	20.772	3.7172	0.0144	0.0041	4.7792	0.9013
22	Dt ~ seedscale + (1|Year))	21.129	8.2615	0.0168	0.0104	4.7449	1.5001
23	Dt ~ sine3 + seedscale + AvgDepthS + (1|Year))	21.486	3.8829	0.0142	0.0042	4.8075	0.9116
24	Dt ~ sine3 + seedscale + ColdDaysJS + (1|Year))	22.775	3.1516	0.0137	0.0033	4.8519	0.7802
25	Dt ~ sine3 + ColdDaysJB + (1|Year))	22.9	6.0087	0.0147	0.0050	4.7649	0.7688
26	Dt ~ sine3 + seedscale + SumPrecipS + (1|Year))	23.159	4.2998	0.0134	0.0043	4.9344	0.9549
27	Dt ~ sine3 + seedscale + GDDPrevS + (1|Year))	25.659	3.2129	0.0122	0.0037	5.1158	0.9395
28	Dt ~ sine3 + seedscale + MeltDays + (1|Year))	26.608	3.2703	0.0119	0.0036	5.1694	0.9274
29	Dt ~ sine3 + (1|Year))	27.602	4.6677	0.0107	0.0042	5.4364	1.0819
30	Dt ~ sine3 + seedscale + LengthS + (1|Year))	27.98	2.7231	0.0115	0.0035	5.2348	0.9393
31	Dt ~ sine3 + seedscale + GDDS + (1|Year))	28.06	3.8080	0.0116	0.0040	5.2415	0.9806
32	Dt ~ sine3 + RainDays + (1|Year))	32.017	1.9831	0.0051	0.0022	6.9379	1.1195

33	Dt ~ sine3 + MeltDaysB + (1|Year))	33.57	0.7986	0.0036	0.0014	7.6239	1.0834
34	Dt ~ 1 + (1|Year))	35.923	4.4000	0.0034	0.0024	8.0056	1.5809
35	Dt ~ sine3 + seedscale + ColdDaysJB + SumPrecip3retavgS + AvgDepth3retavgS + GDD3retavgS + (1|Year))	37.085	5.0374	0.0028	0.0012	8.1540	0.8325
36	Dt ~ sine3 + AvgDepthS + (1|Year))	38.109	1.7076	0.0021	0.0009	8.6689	1.1170
37	Dt ~ sine3 + SumPrecipPrevS + (1|Year))	38.151	2.5967	0.0023	0.0010	8.5643	1.1765
38	Dt ~ sine3 + SprPrecipS + (1|Year))	38.395	2.3273	0.0022	0.0008	8.6258	1.0334
39	Dt ~ sine3 + MeltDays + (1|Year))	38.438	2.8157	0.0022	0.0008	8.5713	1.0115
40	Dt ~ sine3 + SumPrecipS + (1|Year))	39.232	2.7553	0.0021	0.0009	8.6846	1.1444
41	Dt ~ sine3 + IntSnowDepthS + (1|Year))	39.314	1.6960	0.0021	0.0009	8.6940	1.1140
42	Dt ~ sine3 + GDDPrevS + (1|Year))	39.795	2.9543	0.0021	0.0009	8.7214	1.1298
43	Dt ~ sine3 + LengthS + (1|Year))	42.074	2.3345	0.0019	0.0008	8.9002	1.1135
44	Dt ~ sine3 + ColdDaysJS + (1|Year))	42.828	2.0225	0.0018	0.0007	8.9585	1.0307
45	Dt ~ sine3 + GDDS + (1|Year))	43.589	2.1519	0.0018	0.0009	9.0399	1.1735
46	Dt ~ sine3 + seedscale + SumPrecip3retavgS + AvgDepth3retavgS + GDD3retavgS + (1|Year))	45.885	0.7323	0.0008	0.0004	10.6187	1.2658
47	Dt ~ sine3 + SumPrecip3retavgS + AvgDepth3retavgS + GDD3retavgS + (1|Year))	47	0.0000	0.0001	0.0000	15.6203	1.2496

Appendix B. Model ranking structure for early summer analysis.

	Model	Mean Rank	Rank SD	Mean Wt	Wt SD	Mean Delta AIC	Delta AIC SD
Density Dependent Variables							
1	Dt~ PrevHiLo	1.486	1.0941	0.4280	0.2271	0.3255	0.7924
2	Dt ~ Dt-1	2.947	1.4249	0.1232	0.0757	2.8473	1.9562
3	Dt ~ Dt-1 + sine3	4.434	2.2691	0.0936	0.0808	3.6433	2.1920
4	Dt ~ cos2	5.054	2.4834	0.0794	0.0803	4.2601	2.5765
5	Dt ~ 1	5.334	2.1783	0.0597	0.0502	4.7463	2.6143
6	Dt ~ Dt-1 + cos2	5.823	2.1749	0.0571	0.0371	4.4105	1.9785
7	Dt ~ Dt-1 + cos3	6.432	2.1854	0.0500	0.0431	4.8160	2.1835
8	Dt ~ sine3	7.813	2.2066	0.0327	0.0346	6.1611	2.7885
9	Dt ~ Dt-1 + sine3 + cos3	8.04	2.3698	0.0332	0.0329	5.7940	2.3333
10	Dt ~ cos3	8.292	1.9709	0.0290	0.0302	6.4155	2.8689
11	Dt ~ cos3 + sine3	10.345	1.2624	0.0139	0.0151	7.9941	2.9858
Density Dependent Variables + Environmental Variables							
1	Dt ~ PrevHiLo	2.712	1.2492	0.1153	0.0294	1.3227	1.2092
2	Dt ~ PrevHiLo + ColdDays	3.582	2.8955	0.1395	0.0961	1.3142	1.5510
3	Dt ~ PrevHiLo + seedscale	3.638	2.6423	0.1276	0.0877	1.4304	1.4587
4	Dt ~ PrevHiLo + SprPrecip	5.354	2.9919	0.0815	0.0524	2.2415	1.4640
5	Dt ~ PrevHiLo + RainDaysB	5.495	3.3489	0.0907	0.0700	2.1216	1.4194
6	Dt ~ PrevHiLo + RainDays	6.985	3.3815	0.0679	0.0513	2.6238	1.3400
7	Dt ~ PrevHiLo + SumPrecipPrev	9.475	3.6264	0.0556	0.0695	3.1570	1.3753
8	Dt ~ PrevHiLo + MeltDays	9.519	3.0034	0.0456	0.0187	3.2227	1.1869
9	Dt ~ PrevHiLo + MeltDaysB	9.654	2.9952	0.0438	0.0169	3.2918	1.1757
10	Dt ~ PrevHiLo + Length	9.735	3.0991	0.0431	0.0190	3.3481	1.2432
11	Dt ~ PrevHiLo + GDDPrev	9.933	3.3487	0.0427	0.0195	3.3899	1.2980
12	Dt ~ PrevHiLo + ColdDaysB	10.098	3.1794	0.0400	0.0127	3.4633	1.1474
13	Dt ~ PrevHiLo + IntSnowDepth	10.489	2.9439	0.0401	0.0161	3.4968	1.3161
14	Dt ~ PrevHiLo + AvgDepth	10.62	2.8375	0.0397	0.0152	3.5100	1.3016
15	Dt ~ 1	12.711	4.2890	0.0269	0.0369	5.7435	2.9461